Stanislav (Stas) Babak.

AstroParticule et Cosmologie, CNRS (Paris)

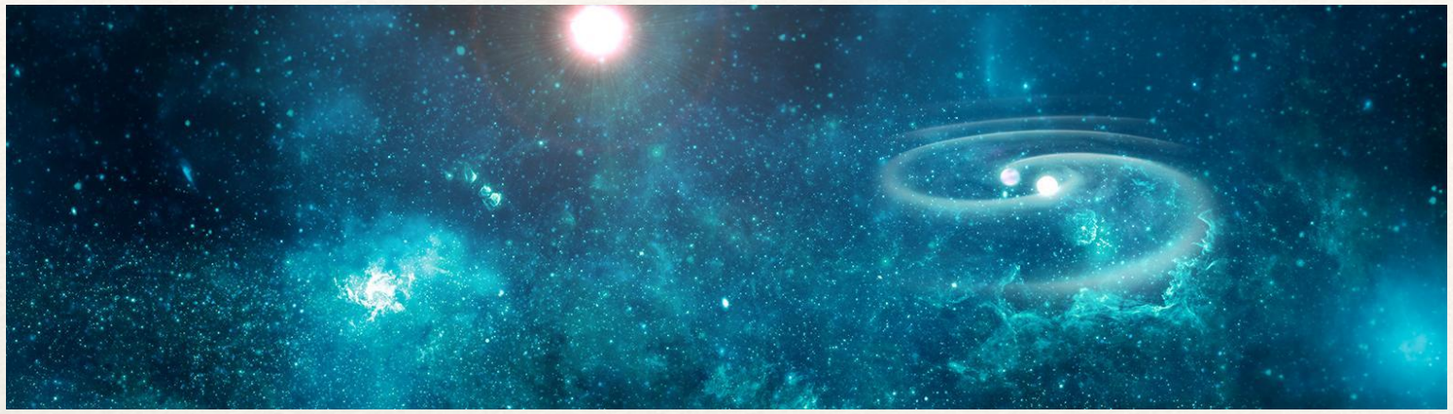

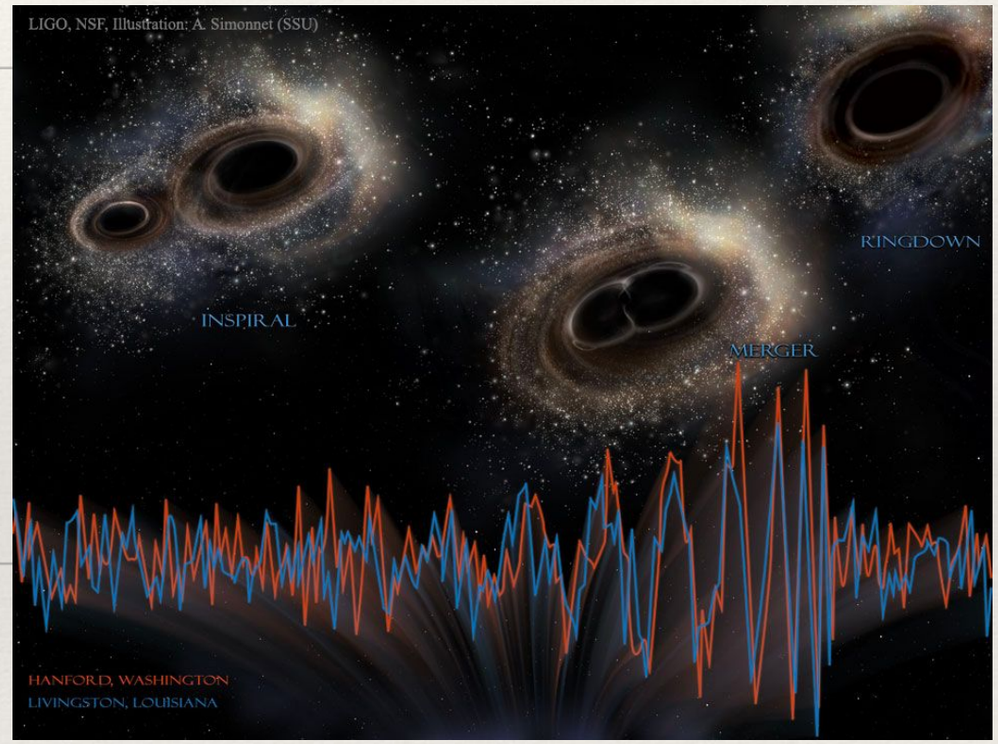

Gravitational wave transient catalogue from O3a

LIGO Scientific Collaboration
and
Virgo Collaboration

7th Kagra International workshop, 18-20 Dec 2020

Outline

- Performance of AdLIGO and AdVirgo during O3a
- Search for coalescing binaries in O3
- Properties of detected gravitational wave (GW) signals

O3a Catalog Paper
dcc.ligo.org/LIGO-P2000061/public
arXiv: 2010.14527

GWTC-2 Data Release
www.gw-openscience.org/GWTC-2/

Companion Papers

Populations: (***Talk by D. Wysocki***)
dcc.ligo.org/LIGO-P2000077/public
arXiv: 2010.14533

Tests of GR:
dcc.ligo.org/LIGO-P2000091/public
arXiv: 2010.14529

GW detector's network

LIGO Hanford
(Washington, USA)

KAGRA (Japan)
joining soon!

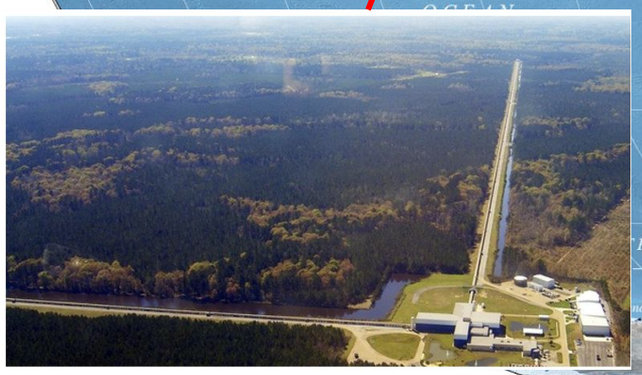

LIGO Livingston
(Louisiana, USA)

Virgo
(Pisa, Italy)

Sensitivity during O3a

BNS range: Median distance to the merging neutron stars (masses 1.5-1.5) binary which produces GW signal with signal-to-noise ratio (SNR) = 8

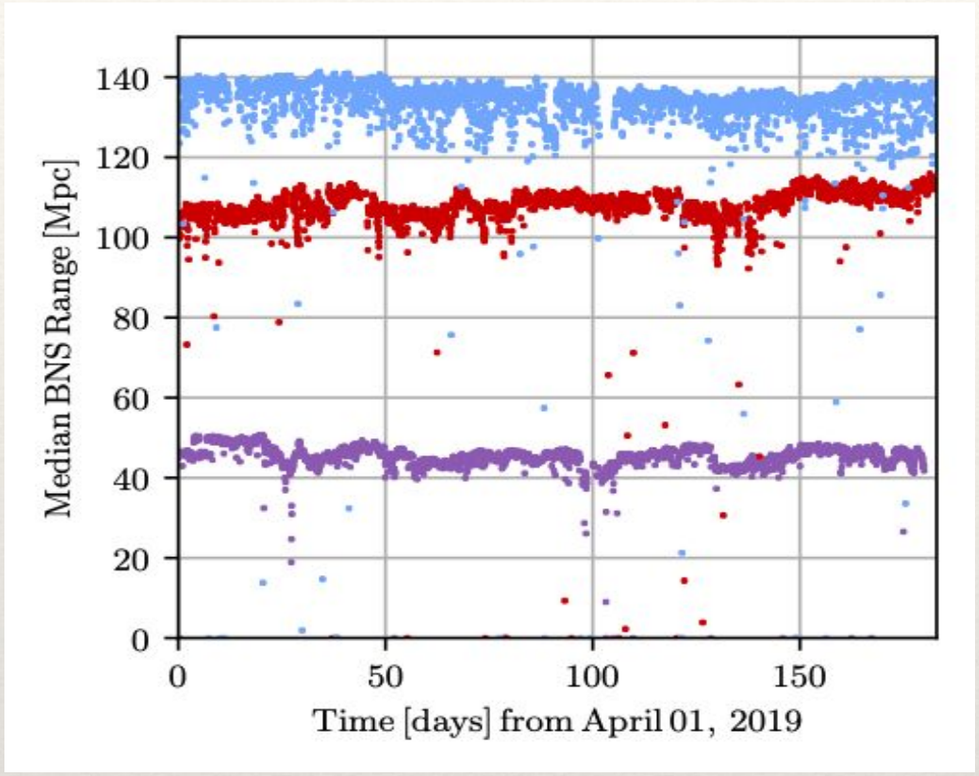

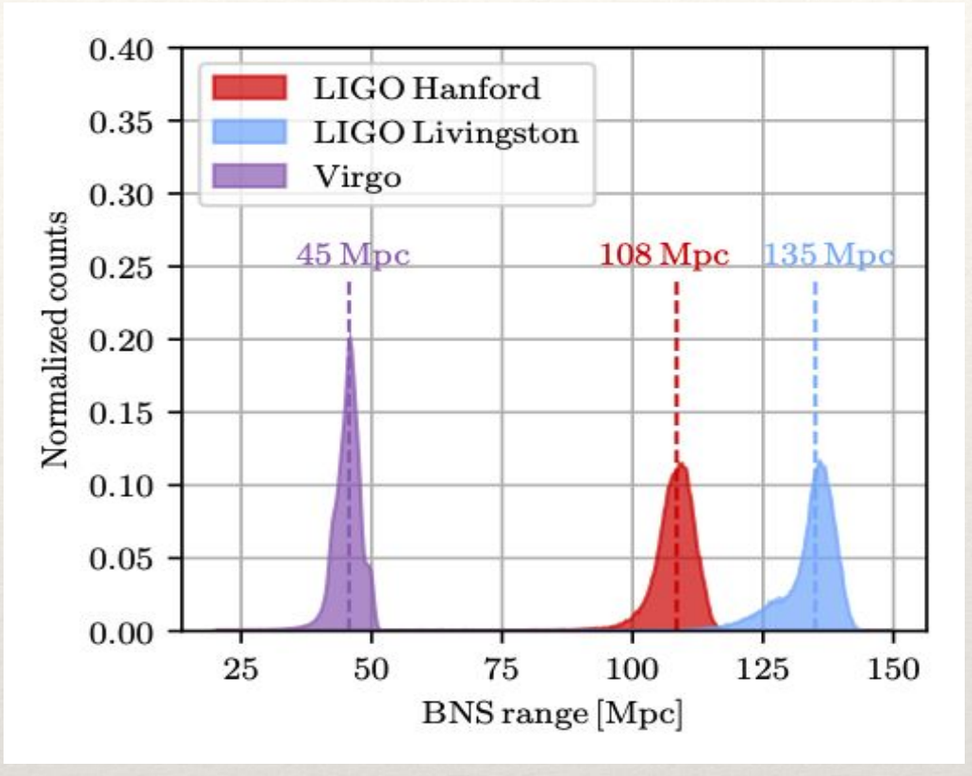

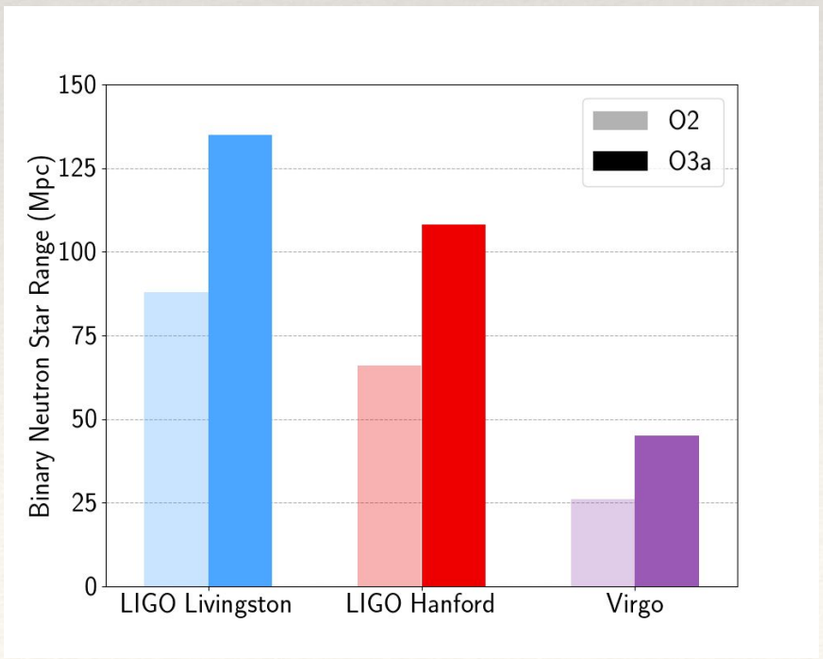

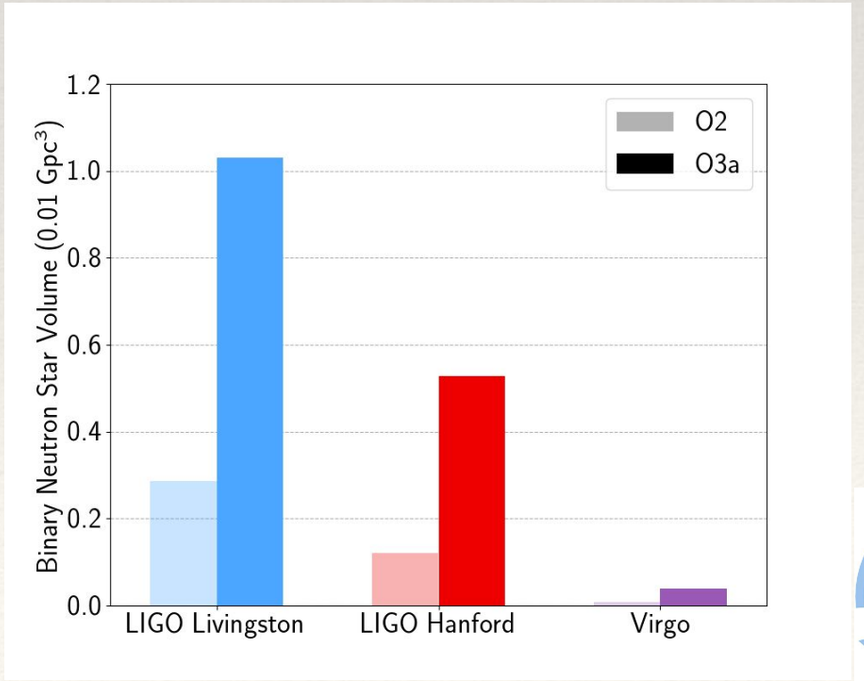

Performance of detectors

Duty factor: Percentage of wall-clock time that detector is in observing mode

O3a	Duty factor (O3/O2)	Uptime
Hanford:	71 / 62%	130 d
Livingston:	76 / 61%	139 d
Virgo:	76 / 80%	140 d

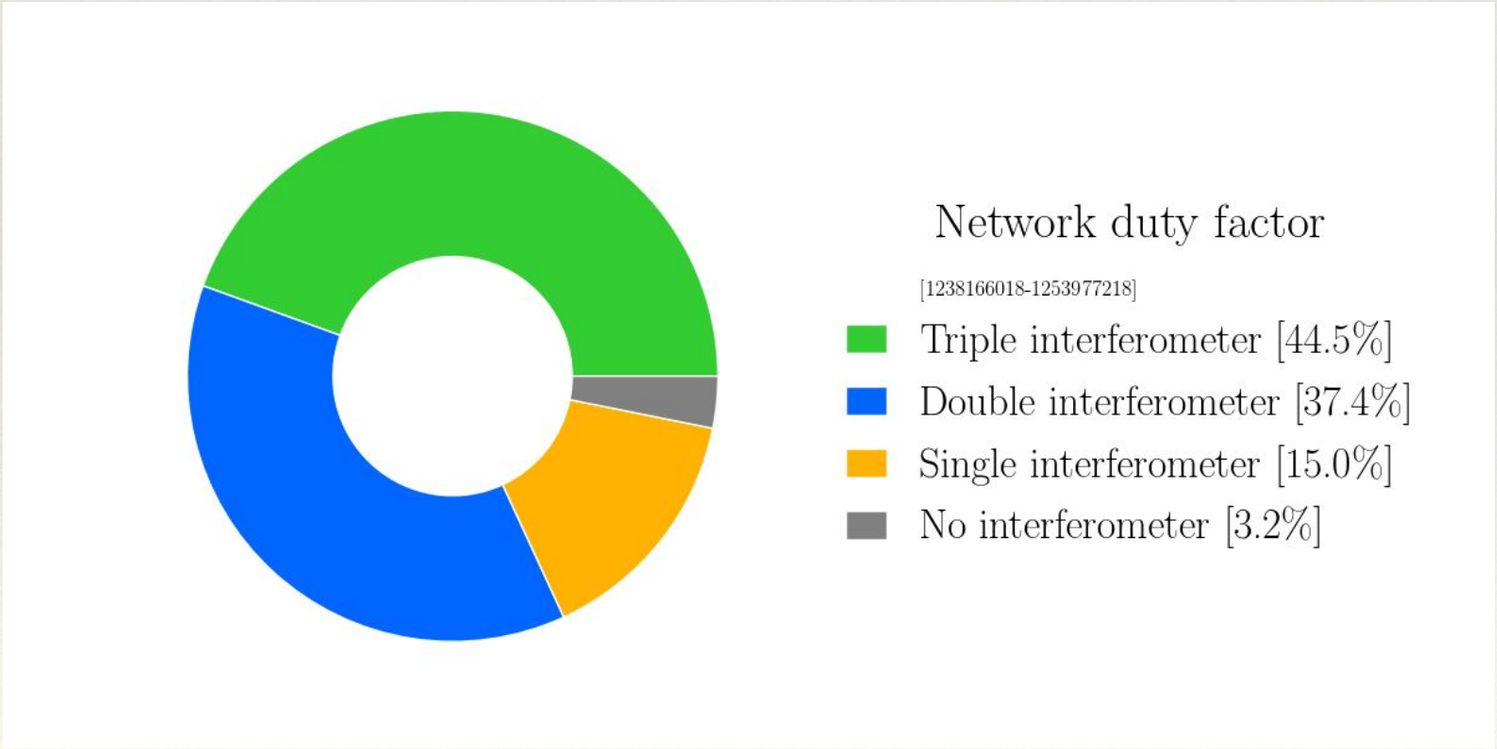

Instrumental artifacts

Glitches: Short duration instrumental artifacts that add excess noise to the interferometer strain data

Common sources of glitches include:

- Scattered laser light
- Thunderclaps
- Earthquakes

When possible, we subtract glitches with the *BayesWave* algorithm near GW candidates for parameter estimation:

- Subtraction excess of power using wavelets decomposition
- Simultaneous fit for glitches and signal

Blip glitches: unknown origin

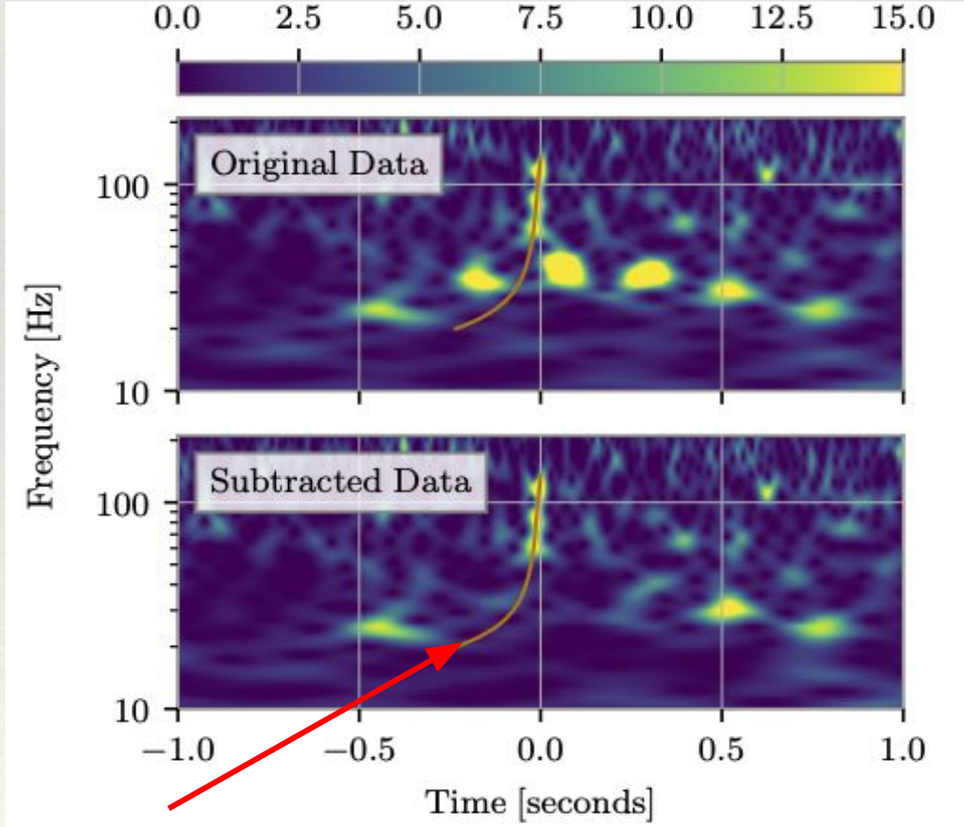

GW 190701_203306

Glitch rate and calibraton

LIGO: increase in the glitch rate, Virgo decrease in glitch rate
Livingston: daily cycle of scattered light - tied to ground motion driven by human activity

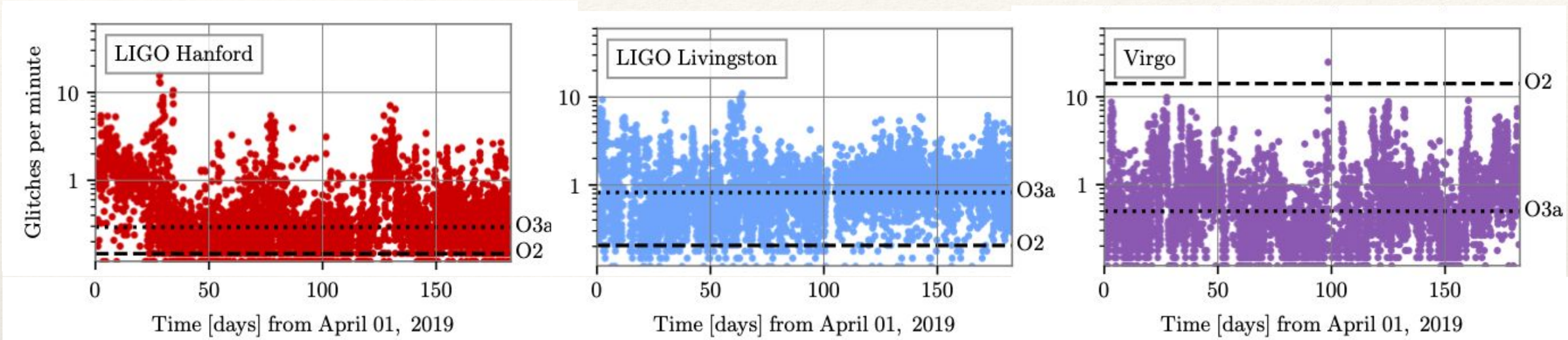

Calibraton uncertainties:

- Transformation of optical readout into GW strain
- A *photon calibrator*, a laser that pushes on the test masses with a known force, is used as an absolute reference

- Modelling systematic uncertainties (spline) and marginalized over in parameter estimation

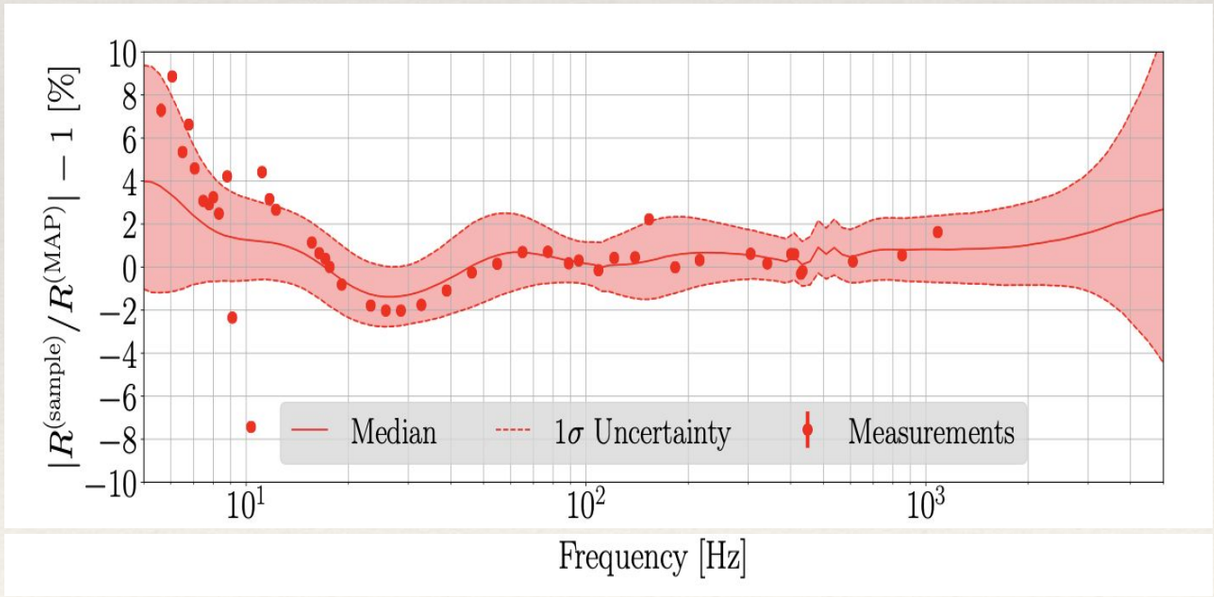

Detection strategy

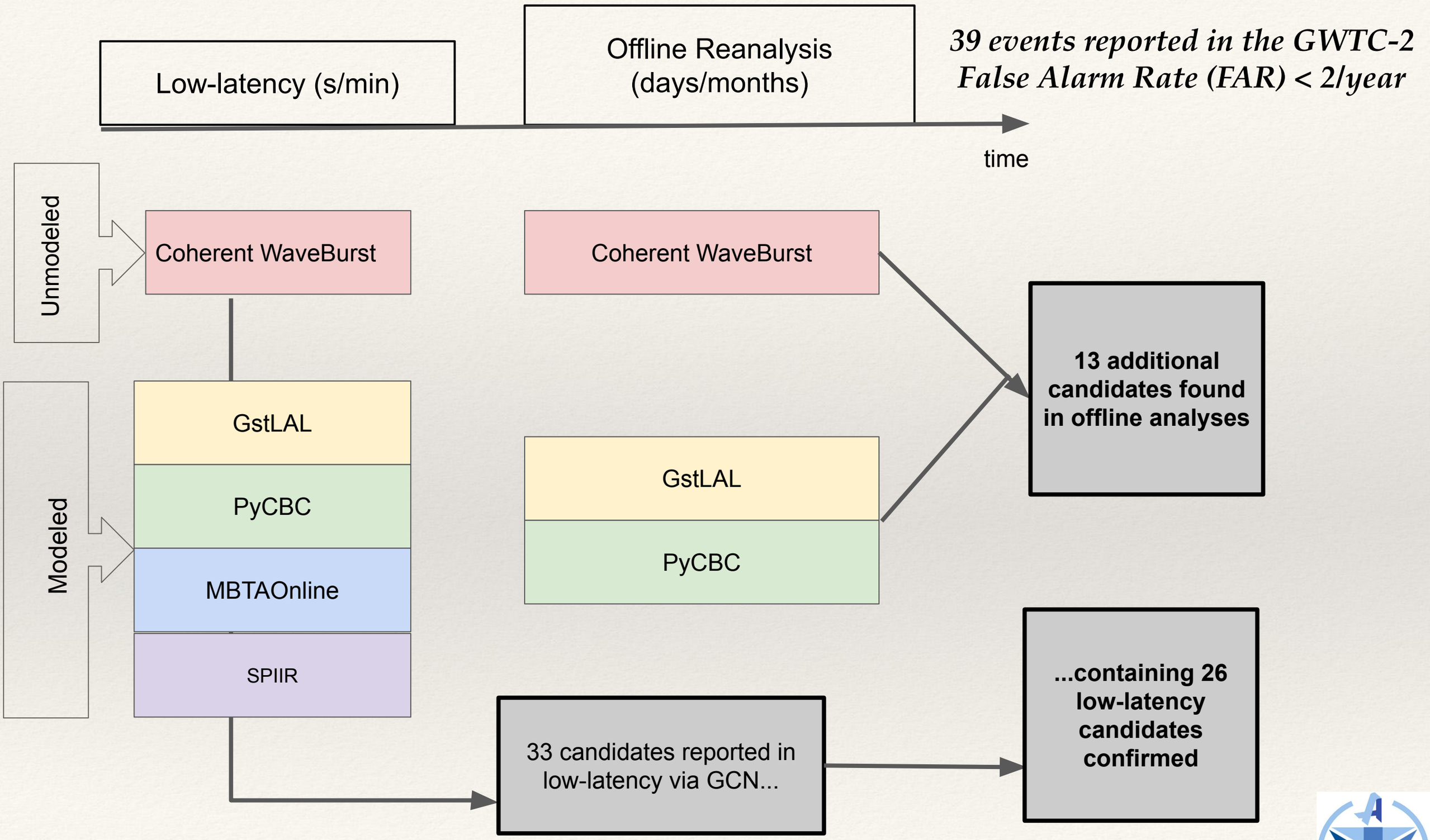

Modelled, grid-based search

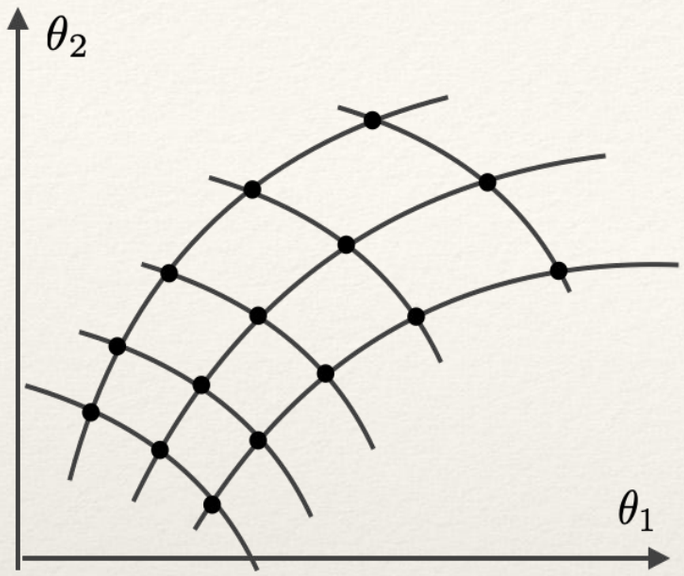

- We want to cover the parameter space (N-dim) by grid of points at equal distance from each other.
- Grid: not too coarse, not too fine
- The distance is determined **not** by a coordinate distance but by "proper" distance — correlation between nearby templates: introduce interval and metric

Assuming the circular orbits

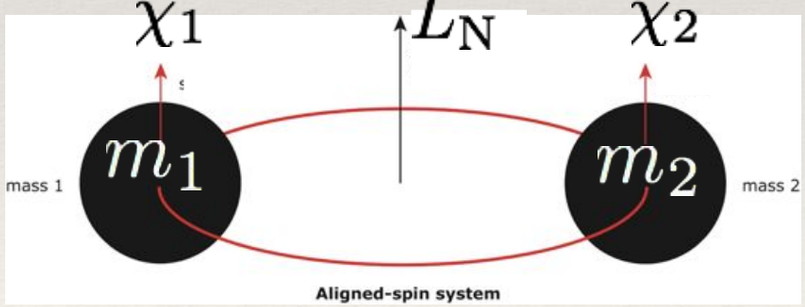

$$\chi_{\rm eff} = \frac{(m_1\vec{\chi}_1 + m_2\vec{\chi}_2)\cdot\hat{L}_N}{M}$$

SNR threshold: 4 in a single detector - basis for GW candidate + GW consistency check + data quality

Template bank for GstLAL

- m_1, m_2: 1 - 400 solar masses
- $m_{\rm total}$: 2 - 758 solar masses
- (Anti-) aligned spin
- ~1.7 million templates

Template bank for PyCBC

- $m_1 > 1$ solar mass
- $m_{\rm total} < 500$ solar masses
- mass ratio < 98
- (Anti-) aligned spin
- ~400,000 templates

Estimating significance of candidates

Events in GWTC-2 passed the false alarm rate (FAR) threshold of **2 per year**. This means we could have up to ~3 false alarms mixed in our event list.

To guide us, we include statistical measures of the false alarm rate and probability of BBH astrophysical origin.

$$\mathrm{FAR} = \frac{N(\Lambda \geq \Lambda^*)}{T}$$

Number N of background events with ranking statistic Λ higher than Λ^* over experiment time T

$p_{\text{astro-}}$ for events consistent with BBH from Poisson mixture model formalism

Farr,et al. Physical Review D (2015)

Summary of GW events

- Candidate events highlighted in red are the most likely to be noise.
- The candidate with the highest FAR is GW190426. It was previously reported in low-latency as a possible neutron star-black hole event.
- Candidates in bold were not previously reported.
- Candidate events highlighted in yellow were found in only one detector. Thus they have larger uncertainties in the FAR.

Name	Inst.	cWB		GstLAL			PyCBC			PyCBC BBH		
		FAR (yr^{-1})	SNR*	FAR (yr^{-1})	SNR	p_{astro}	FAR (yr^{-1})	SNR*	p_{astro}	FAR (yr^{-1})	SNR*	p_{astro}
GW190408_181802	HLV	$< 9.5 \times 10^{-4}$	14.8	$< 1.0 \times 10^{-5}$	14.7	1.00	$< 2.5 \times 10^{-5}$	13.5	1.00	$< 7.9 \times 10^{-5}$	13.6	1.00
GW190412	HLV	$< 9.5 \times 10^{-4}$	19.7	$< 1.0 \times 10^{-5}$	18.9	1.00	$< 3.1 \times 10^{-5}$	17.9	1.00	$< 7.9 \times 10^{-5}$	17.8	1.00
GW190413_052954	HLV	–	–	–	–	–	–	–	–	7.2×10^{-2}	8.6	0.98
GW190413_134308	HLV	–	–	3.8×10^{-1}	10.0	0.95	–	–	–	4.4×10^{-2}	9.0	0.98
GW190421_213856	HL	3.0×10^{-1}	9.3	7.7×10^{-4}	10.6	1.00	1.9×10^{0}	10.2	0.89	6.6×10^{-3}	10.2	1.00
GW190424_180648	L			$7.8 \times 10^{-1\dagger}$	10.0	0.91						
GW190425	LV			$7.5 \times 10^{-4\dagger}$	13.0	–						
GW190426_152155	HLV	–	–	1.4×10^{0}	10.1	–	–	–	–	–	–	–
GW190503_185404	HLV	1.8×10^{-3}	11.5	$< 1.0 \times 10^{-5}$	12.1	1.00	3.7×10^{-2}	12.2	1.00	$< 7.9 \times 10^{-5}$	12.2	1.00
GW190512_180714	HLV	8.8×10^{-1}	10.7	$< 1.0 \times 10^{-5}$	12.3	1.00	3.8×10^{-5}	12.2	1.00	$< 5.7 \times 10^{-5}$	12.2	1.00
GW190513_205428	HLV	–	–	$< 1.0 \times 10^{-5}$	12.3	1.00	3.7×10^{-4}	11.8	1.00	$< 5.7 \times 10^{-5}$	11.9	1.00
GW190514_065416	HL	–	–	–	–	–	–	–	–	5.3×10^{-1}	8.3	0.96
GW190517_055101	HLV	6.5×10^{-3}	10.7	9.6×10^{-4}	10.6	1.00	1.8×10^{-2}	10.4	1.00	$< 5.7 \times 10^{-5}$	10.2	1.00
GW190519_153544	HLV	3.1×10^{-4}	14.0	$< 1.0 \times 10^{-5}$	12.0	1.00	$< 1.8 \times 10^{-5}$	13.0	1.00	$< 5.7 \times 10^{-5}$	13.0	1.00
GW190521	HLV	2.0×10^{-4}	14.4	1.2×10^{-3}	14.7	1.00	1.1×10^{0}	12.6	0.93	–	–	–
GW190521_074359	HL	$< 1.0 \times 10^{-4}$	24.7	$< 1.0 \times 10^{-5}$	24.4	1.00	$< 1.8 \times 10^{-5}$	24.0	1.00	$< 5.7 \times 10^{-5}$	24.0	1.00
GW190527_092055	HL	–	–	6.2×10^{-2}	8.9	0.99	–	–	–	–	–	–
GW190602_175927	HLV	1.5×10^{-2}	11.1	1.1×10^{-5}	12.1	1.00	–	–	–	1.5×10^{-2}	11.4	1.00
GW190620_030421	LV			$2.9 \times 10^{-3\dagger}$	10.9	1.00						
GW190630_185205	LV			$< 1.0 \times 10^{-5}$	15.6	1.00						
GW190701_203306	HLV	5.5×10^{-1}	10.2	1.1×10^{-2}	11.6	1.00	–	–	–	–	–	–
GW190706_222641	HLV	$< 1.0 \times 10^{-3}$	12.7	$< 1.0 \times 10^{-5}$	12.3	1.00	6.7×10^{-5}	11.7	1.00	$< 4.6 \times 10^{-5}$	12.3	1.00
GW190707_093326	HL	–	–	$< 1.0 \times 10^{-5}$	13.0	1.00	$< 1.0 \times 10^{-5}$	12.8	1.00	$< 4.6 \times 10^{-5}$	12.8	1.00
GW190708_232457	LV			$2.8 \times 10^{-5\dagger}$	13.1	1.00						
GW190719_215514	HL	–	–	–	–	–	–	–	–	1.6×10^{0}	8.0	0.82
GW190720_000836	HLV	–	–	$< 1.0 \times 10^{-5}$	11.7	1.00	$< 2.0 \times 10^{-5}$	10.6	1.00	$< 3.7 \times 10^{-5}$	10.5	1.00
GW190727_060333	HLV	8.8×10^{-2}	11.4	$< 1.0 \times 10^{-5}$	12.3	1.00	3.5×10^{-3}	11.5	1.00	$< 3.7 \times 10^{-5}$	11.8	1.00
GW190728_064510	HLV	–	–	$< 1.0 \times 10^{-5}$	13.6	1.00	$< 1.6 \times 10^{-5}$	13.4	1.00	$< 3.7 \times 10^{-5}$	13.4	1.00
GW190731_140936	HL	–	–	2.1×10^{-1}	8.5	0.97	–	–	–	2.8×10^{-1}	8.2	0.96
GW190803_022701	HLV	–	–	3.2×10^{-2}	9.0	0.99	–	–	–	2.7×10^{-2}	8.6	0.99
GW190814	LV			$< 1.0 \times 10^{-5}$	22.2	1.00						
GW190828_063405	HLV	$< 9.6 \times 10^{-4}$	16.6	$< 1.0 \times 10^{-5}$	16.0	1.00	$< 1.5 \times 10^{-5}$	15.3	1.00	$< 3.3 \times 10^{-5}$	15.3	1.00
GW190828_065509	HLV	–	–	$< 1.0 \times 10^{-5}$	11.1	1.00	5.8×10^{-5}	10.8	1.00	$< 3.3 \times 10^{-5}$	10.8	1.00
GW190909_114149	HL	–	–	1.1×10^{0}	8.5	0.89	–	–	–	–	–	–
GW190910_112807	LV			$1.9 \times 10^{-5\dagger}$	13.4	1.00						
GW190915_235702	HLV	$< 1.0 \times 10^{-3}$	12.3	$< 1.0 \times 10^{-5}$	13.1	1.00	8.6×10^{-4}	13.0	1.00	$< 3.3 \times 10^{-5}$	12.7	1.00
GW190924_021846	HLV	–	–	$< 1.0 \times 10^{-5}$	13.2	1.00	$< 6.3 \times 10^{-5}$	12.5	1.00	$< 3.3 \times 10^{-5}$	12.4	1.00
GW190929_012149	HLV	–	–	2.0×10^{-2}	9.9	1.00	–	–	–	–	–	–
GW190930_133541	HL	–	–	5.8×10^{-1}	10.0	0.92	3.4×10^{-2}	9.7	1.00	3.3×10^{-2}	9.8	0.99

Waveform modelling

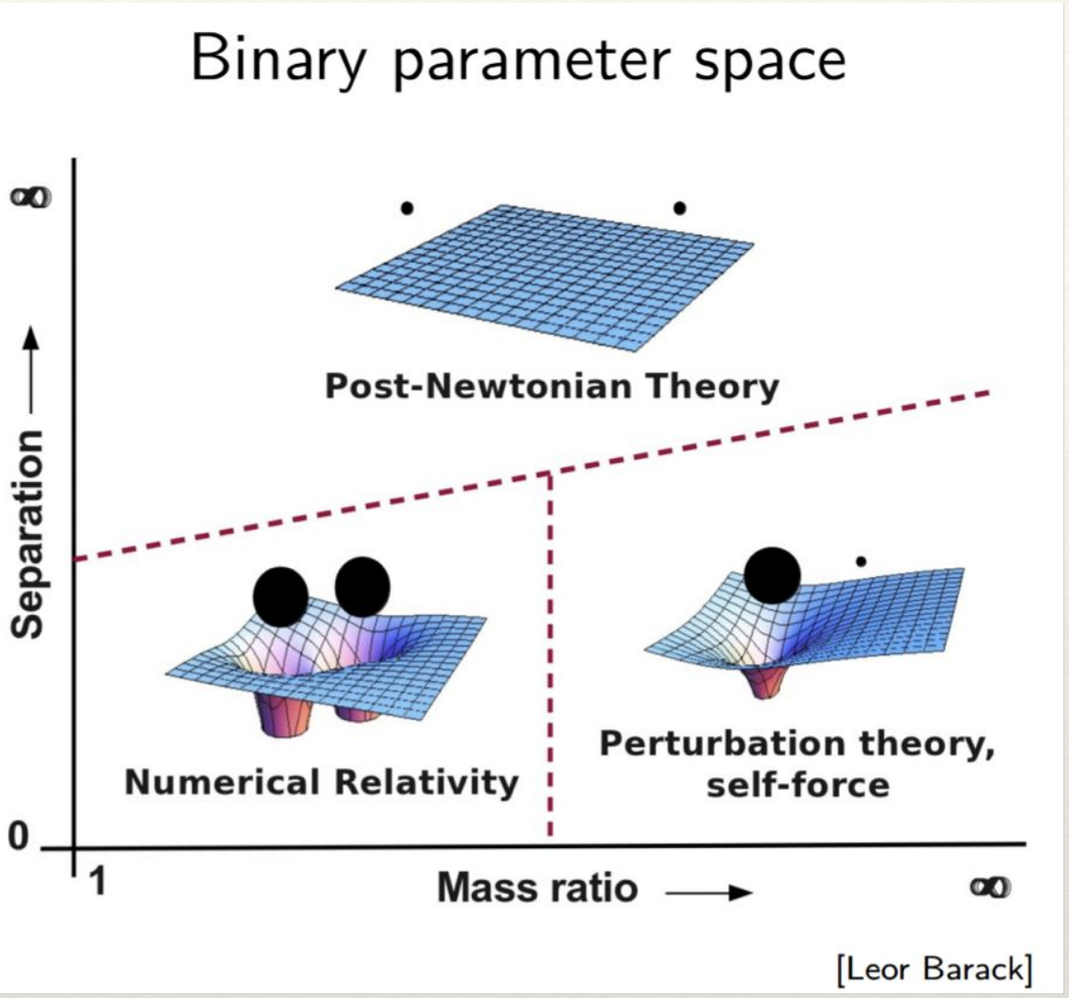

- We have observed only few last cycles (heavy system)
- Merger: requires Numerical Relativity

- NRsurrogate: are built directly by interpolating NR simulations.
- Highly accurate but limited in parameter space and in lenght (~20 orbits)

[Varma et.al. 2019]

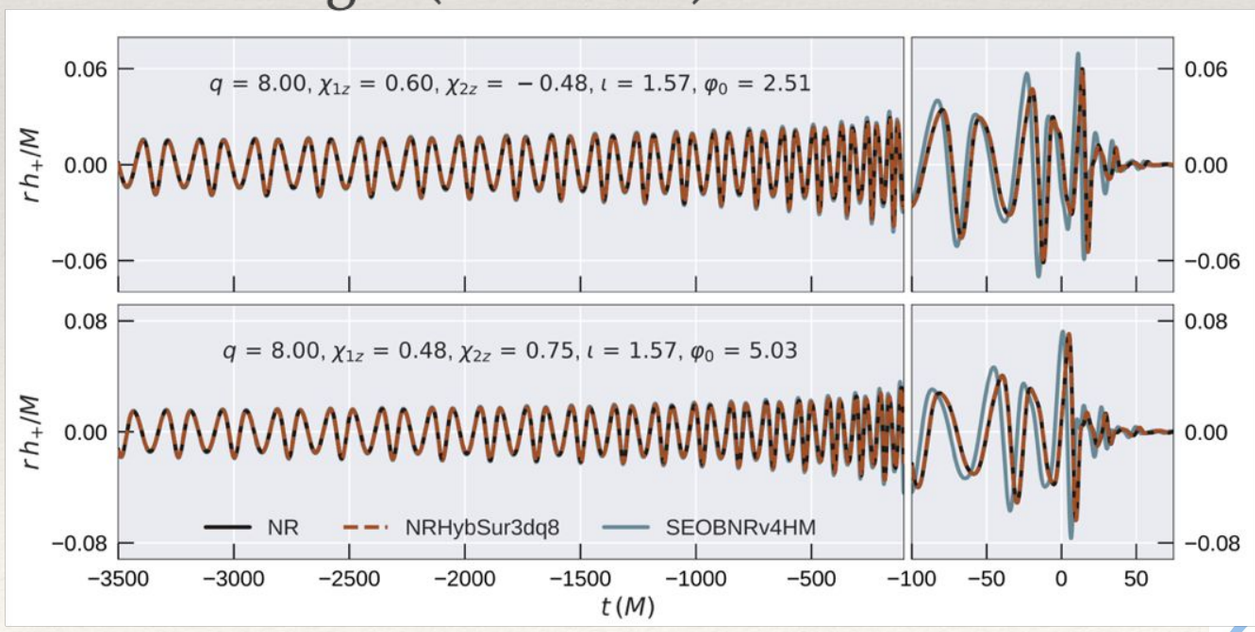

X

Waveform modelling

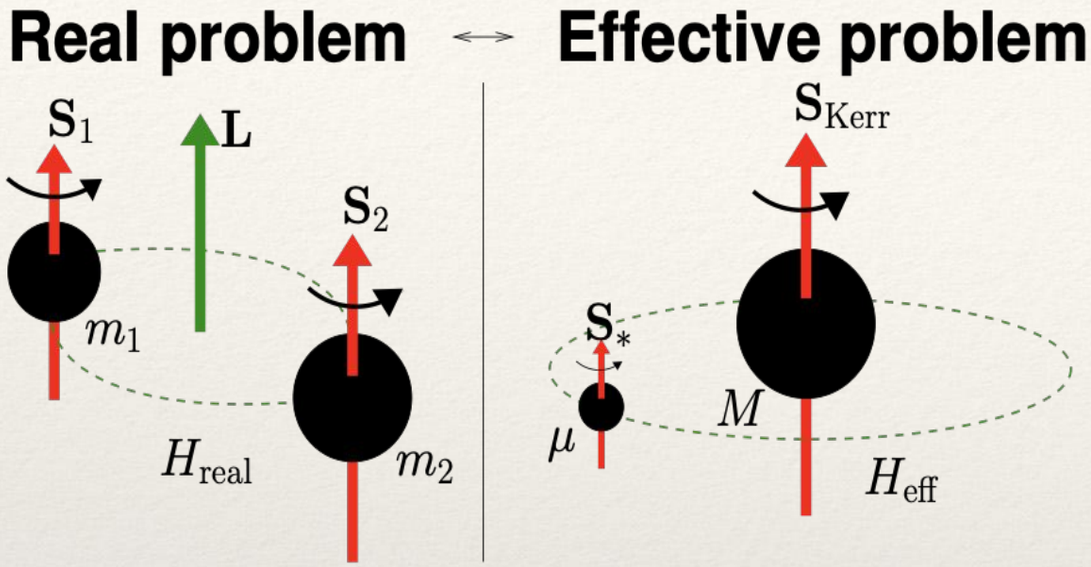

EOB

[Buonanno & Damour 2000]

Effective-One-Body approach:
mapping real two body dynamics onto
motion of a test mass in the s/t of a deformed BH

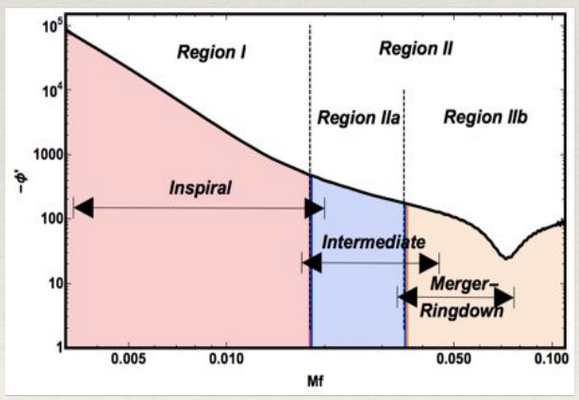

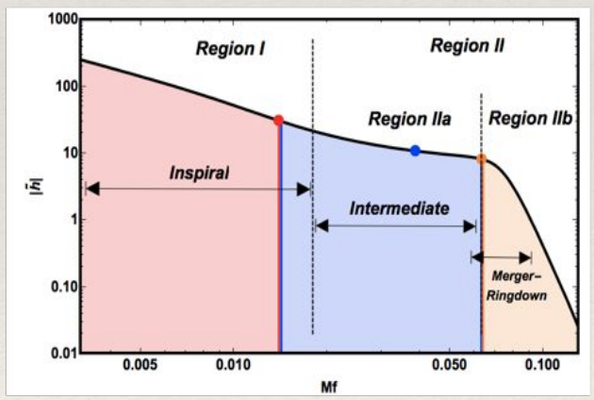

IMRPhenom

Phenomenological model:
uses PN at low frequency + analytic fit for merger
Generated in frequency, very fast

[Khan et al. 2018-2019; García-Quíros et al. 2020, Pratten et al. 2020]

Precession and higher order modes

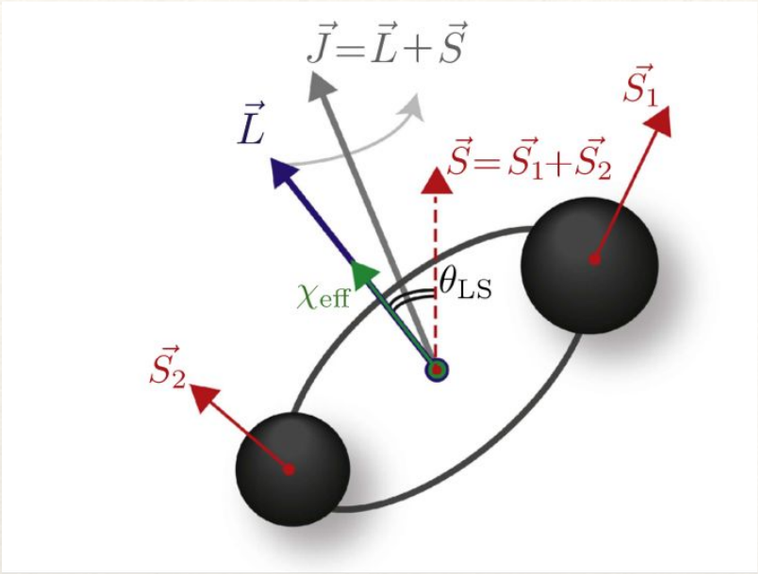

Credit: Carl Rodriguez

- If spins are not aligned wrt orbital angular momentum:
  - orbital precession around total momentum
- Signal = superposition of orbital harmonics,
  - dominant is 2 x orb. freq.
  - subdominant: higher order modes - beyond quadrupolar approximation

[Babak et al. 2016; Cotesta et al. 2018, 2020, Ossokine et al. 2020]

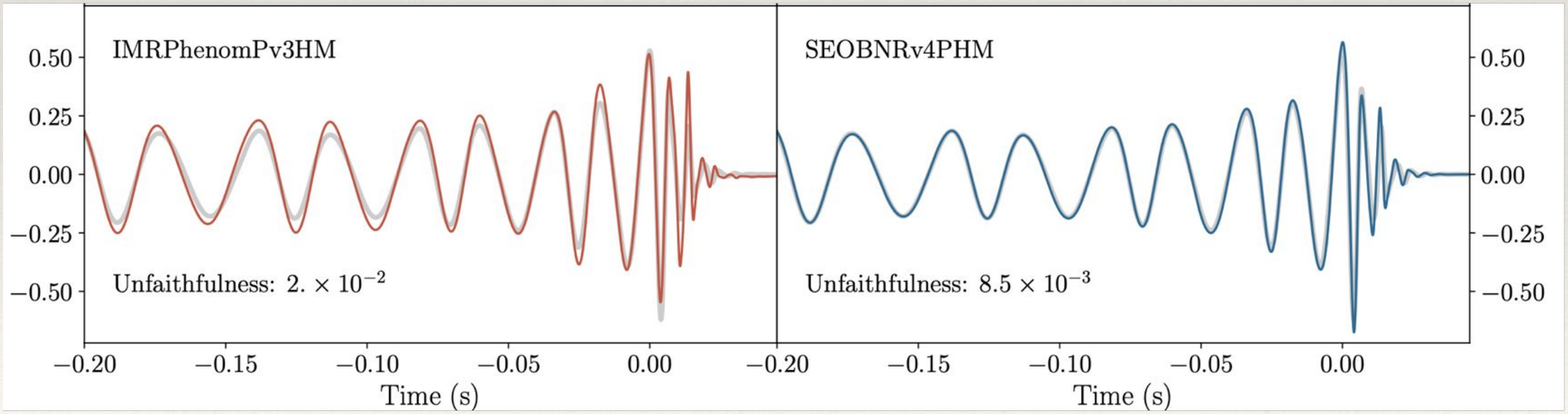

[Khan et al. 2020]

Waveform inventory

Combined key	Waveform name	Precession	Multipoles $(\ell, \lvert m\rvert)$
ZeroSpinIMR*	IMRPhenomD	×	(2, 2)
AlignedSpinIMR	SEOBNRv4_ROM	×	(2, 2)
AlignedSpinIMRHM	IMRPhenomHM	×	(2, 2), (2, 1), (3, 3), (3, 2), (4, 4), (4, 3)
	SEOBNRv4HM_ROM	×	(2, 2), (2, 1), (3, 3), (4, 4), (5, 5)
PrecessingSpinIMR	SEOBNRv4P	✓	(2, 2), (2, 1)
	IMRPhenomPv2	✓	(2, 2)
PrecessingSpinIMRHM	IMRPhenomPv3HM	✓	(2, 2), (2, 1), (3, 3), (3, 2), (4, 4), (4, 3)
	NRSur7dq4	✓	$\ell \leq 4$
	SEOBNRv4PHM	✓	(2, 2), (2, 1), (3, 3), (4, 4), (5, 5)
AlignedSpinTidal†	IMRPhenomD_NRTidal	×	(2, 2)
	TEOBResumS	×	(2, 2)
	SEOBNRv4T_surrogate	×	(2, 2)
PrecessingSpinIMRTidal†	IMRPhenomP_NRTidal	✓	(2, 2)
AlignedSpinInspiralTidal†	TaylorF2	×	(2, 2)
AlignedSpinIMRTidal_NSBH	SEOBNRv4_ROM_NRTidalv2_NSBH	×	(2, 2)
	IMRPhenomNSBH	×	(2, 2)

with matter

Matched filtering and parameter estimation

noise = data - signal

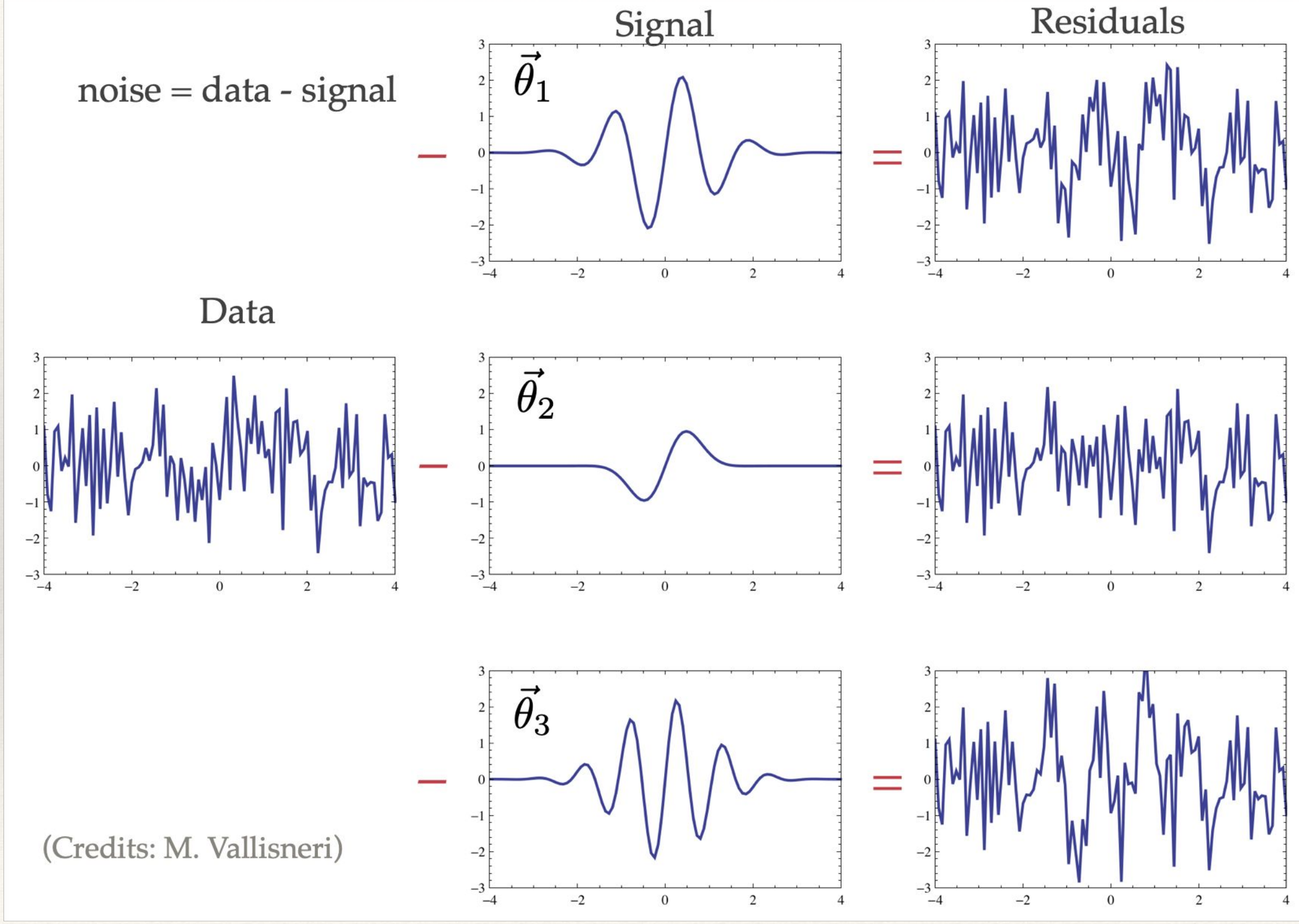

(Credits: M. Vallisneri)

Matched filtering and parameter estimation

noise = data - signal

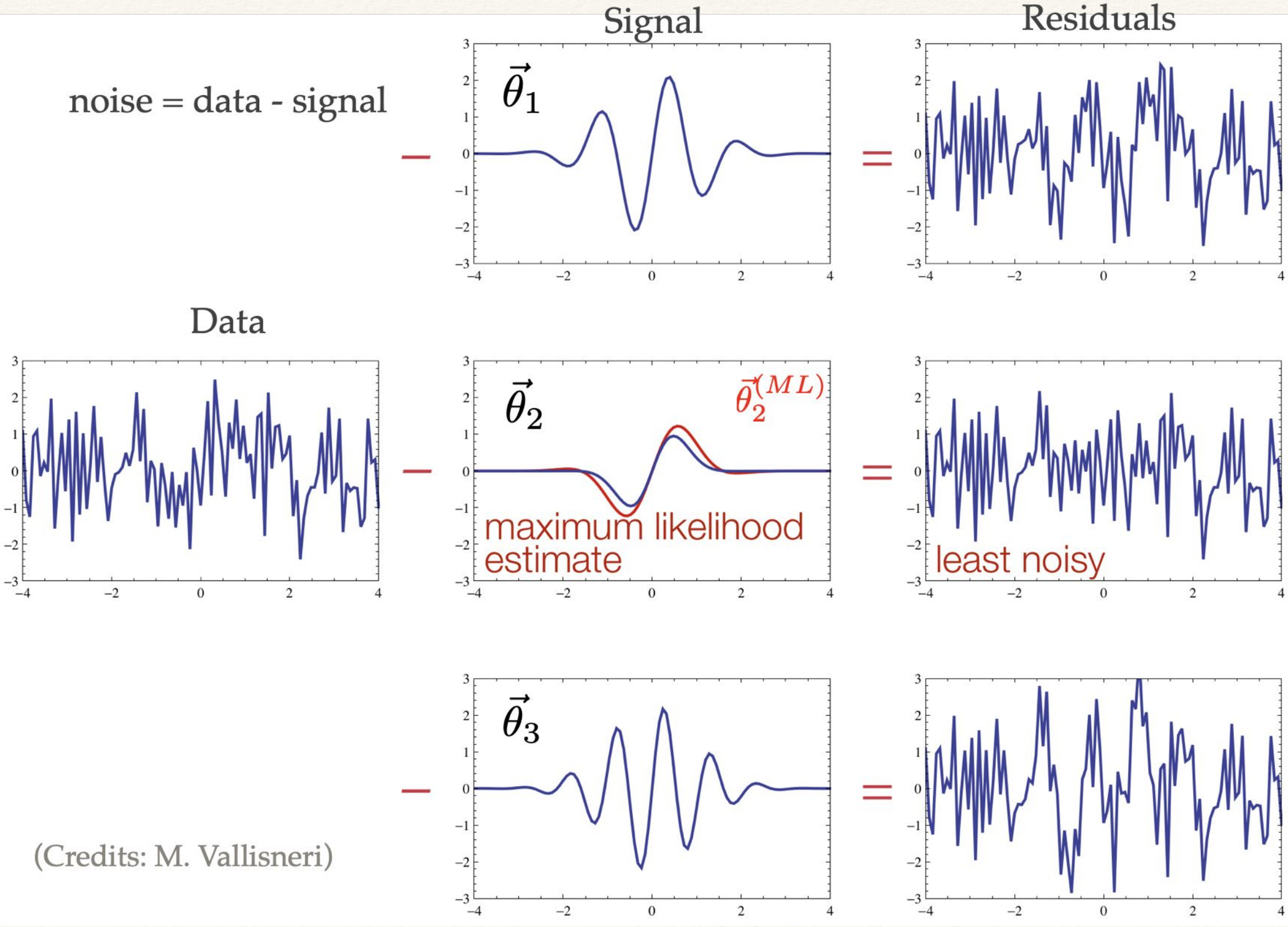

(Credits: M. Vallisneri)

Bayesian approach

Likelihood

Prior

$$p(\theta|d) = \frac{p(d|\theta)\,p(\theta)}{p(d)}$$

Posterior

Evidence

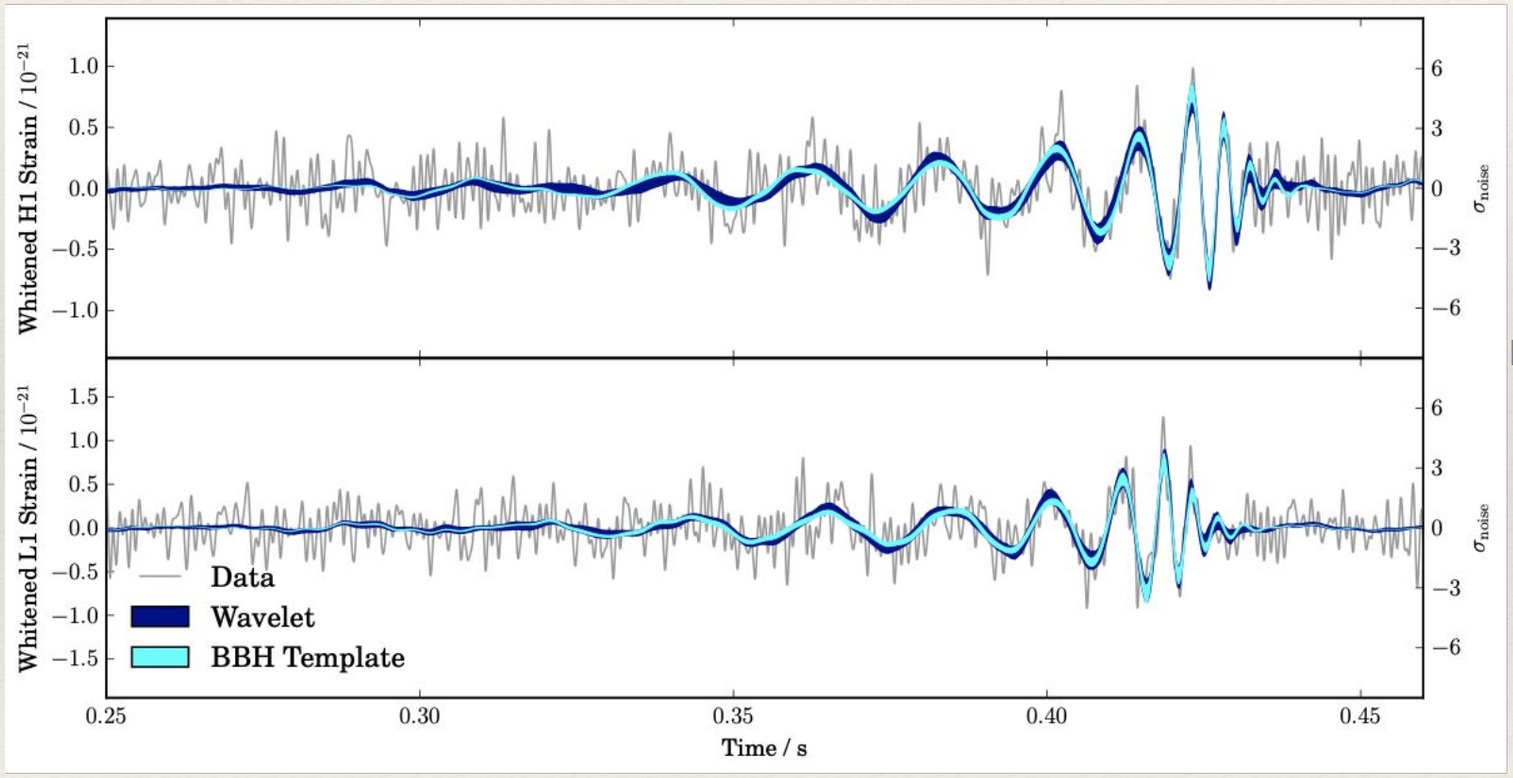

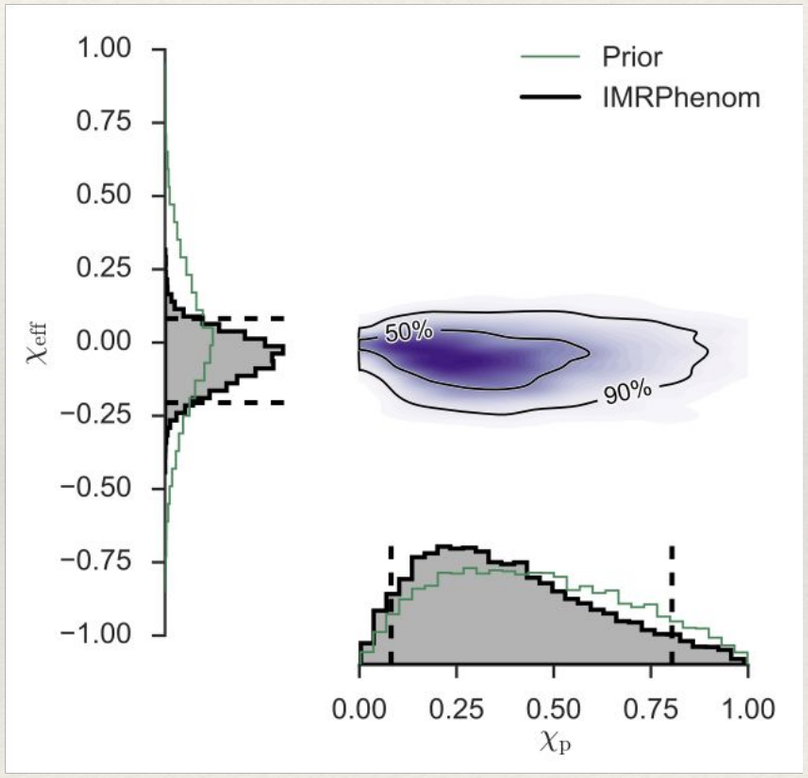

[GW150914, LSC+VIRGO PRL (2016)]

Source parameters

- ***LALInference, Bilby,*** and ***RIFT*** samplers used to produce posterior samples.

- Fiducial results are combined posteriors under different waveform models.

- Posterior samples from all runs are now publicly available.

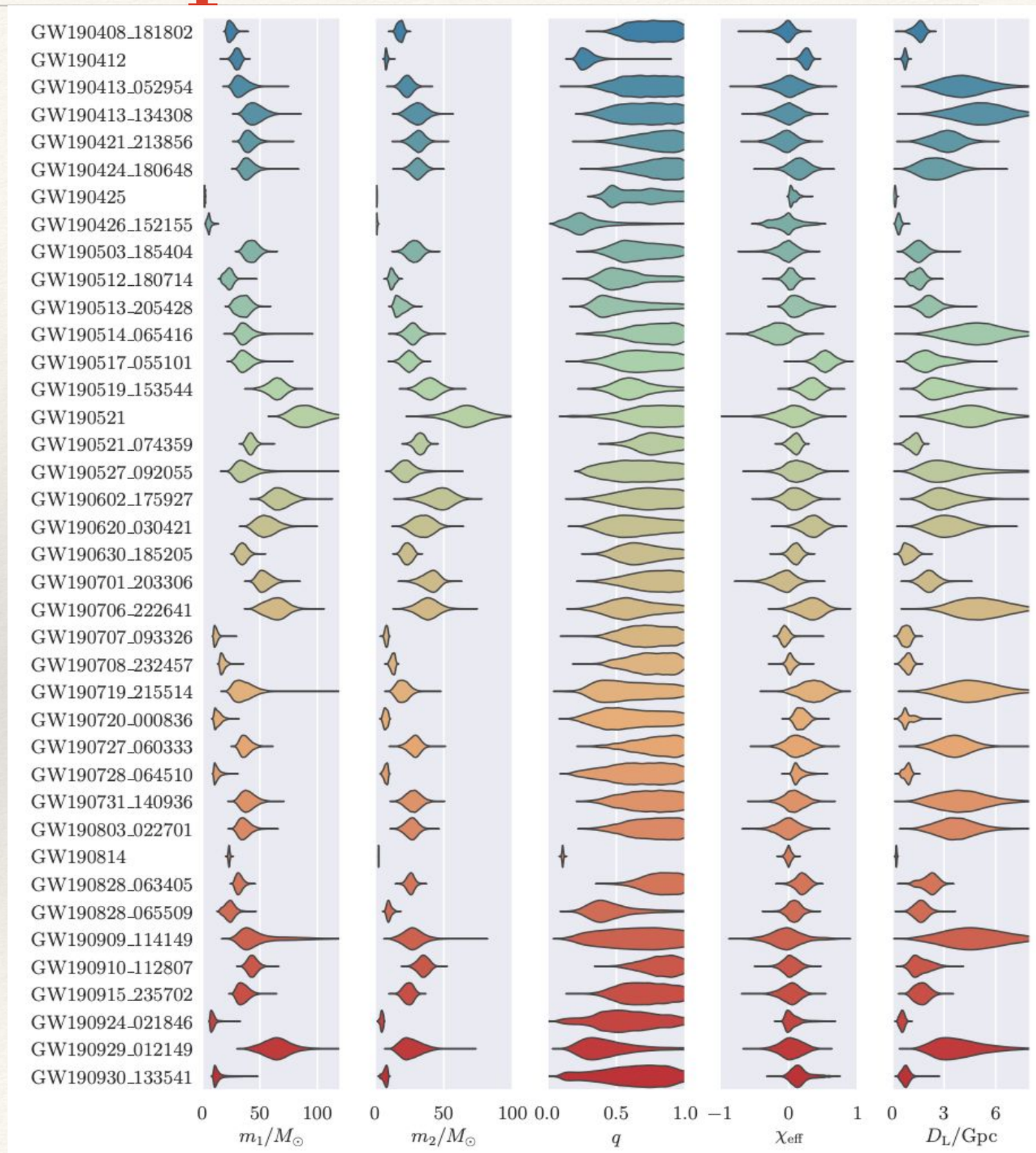

Source parameters

Equal masses

Unequal masses

mass ratio q

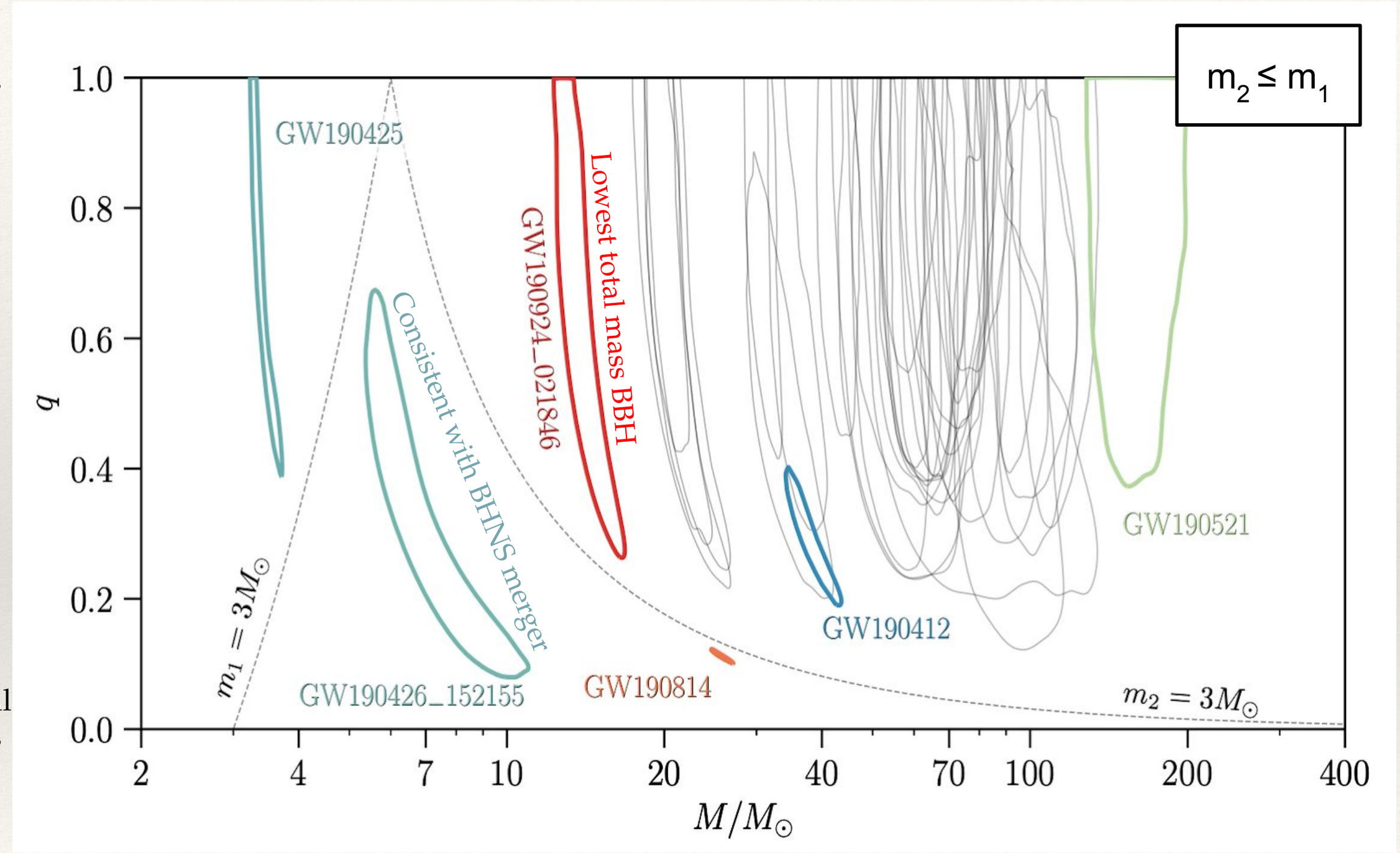

total (source) mass (solar masses)

Spins

Left (right) halves of the circles are shaded in proportion to posterior on spin magnitude and tilt of the more (less) massive component

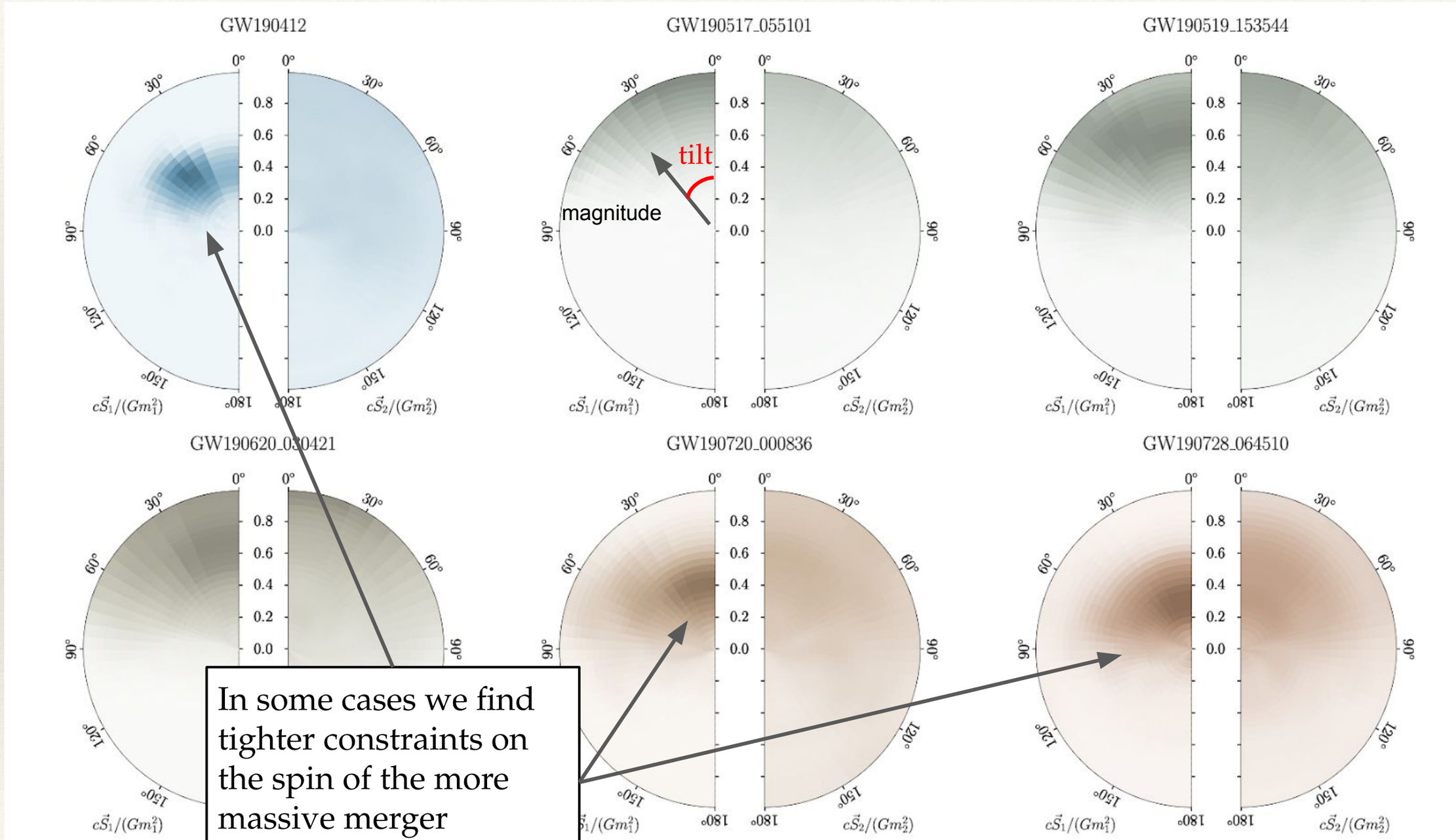

In some cases we find tighter constraints on the spin of the more massive merger component.

Precession?

- A few systems where posterior on effective precession spin parameter χ_p (measure of spin in orbital plane) differs from the prior.
- More massive component in source of GW190814 has small spin magnitude, and therefore we infer small effective precession spin parameter.
- Mild evidence for spin precession in sources of GW190412 and GW190521.
- No systems with strong evidence of precession with the models considered in this work.

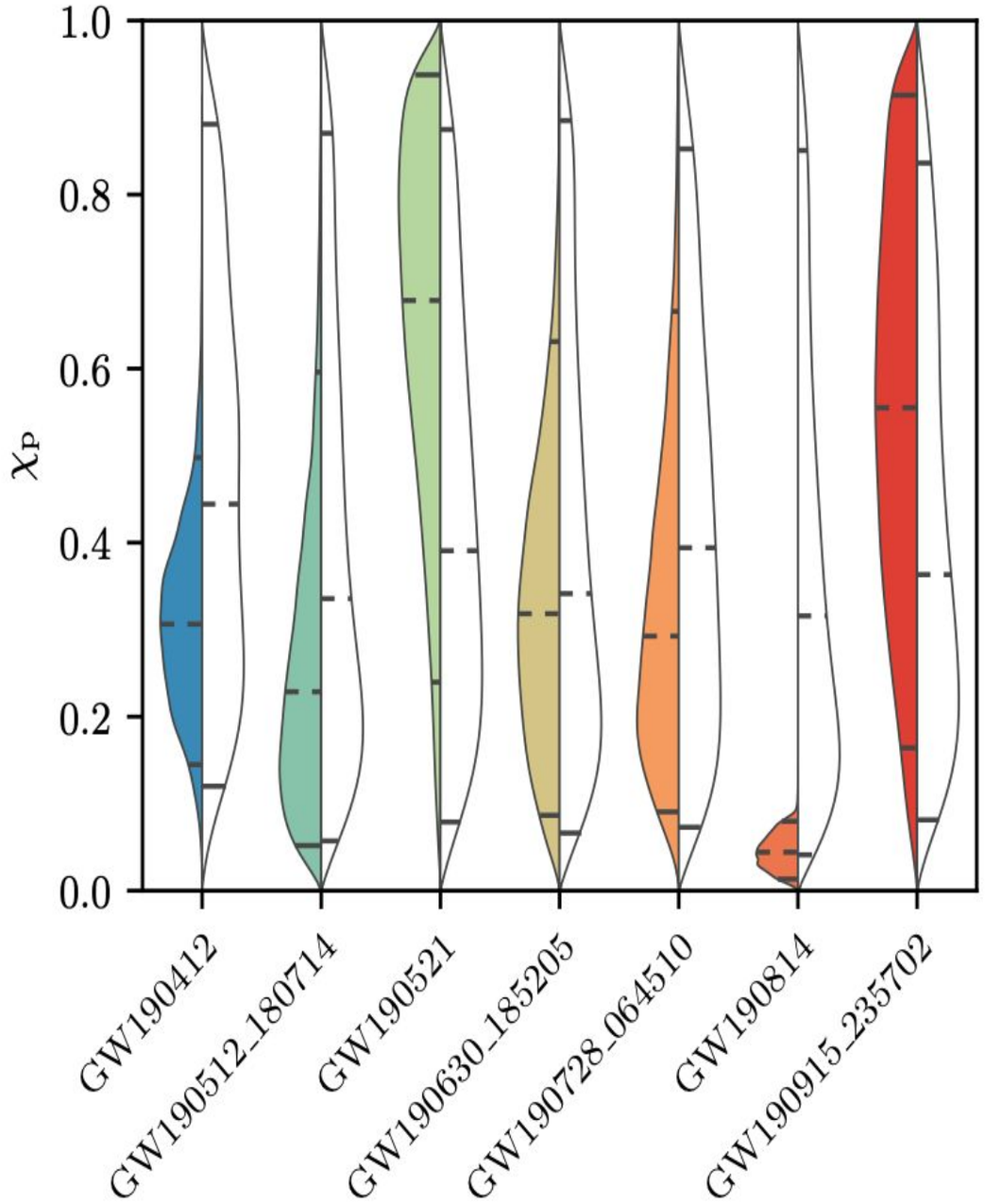

LVC Catalog paper, arXiv: 2010.14527

GW190412

LVC 2020 GW190412

Parameter[a]	EOBNR PHM	Phenom PHM	Combined
$m_1/M_\odot$	$31.7^{+3.6}_{-3.5}$	$28.1^{+4.8}_{-4.3}$	$30.1^{+4.6}_{-5.3}$
$m_2/M_\odot$	$8.0^{+0.9}_{-0.7}$	$8.8^{+1.5}_{-1.1}$	$8.3^{+1.6}_{-0.9}$
$M/M_\odot$	$39.7^{+3.0}_{-2.8}$	$36.9^{+3.7}_{-2.9}$	$38.4^{+3.8}_{-3.9}$

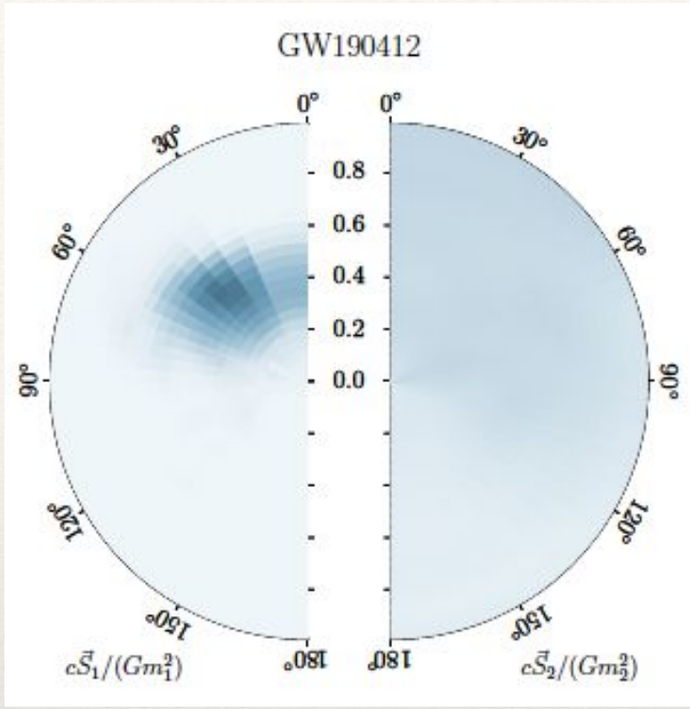

- Log_{10}(Bayes factor) > 3 in favour of higher order modes (beyond quadrupole)
- Tilt angle ~45.8 deg, χ_1~ 0.44
- Good localization ~21 deg^2, $V_{90\%}$ ~ 0.037Gpc^3
- Questions of formation: densed env., triple or quadruple system, evolution in AGN disk

GW190425

LVC, 2020 GW190425

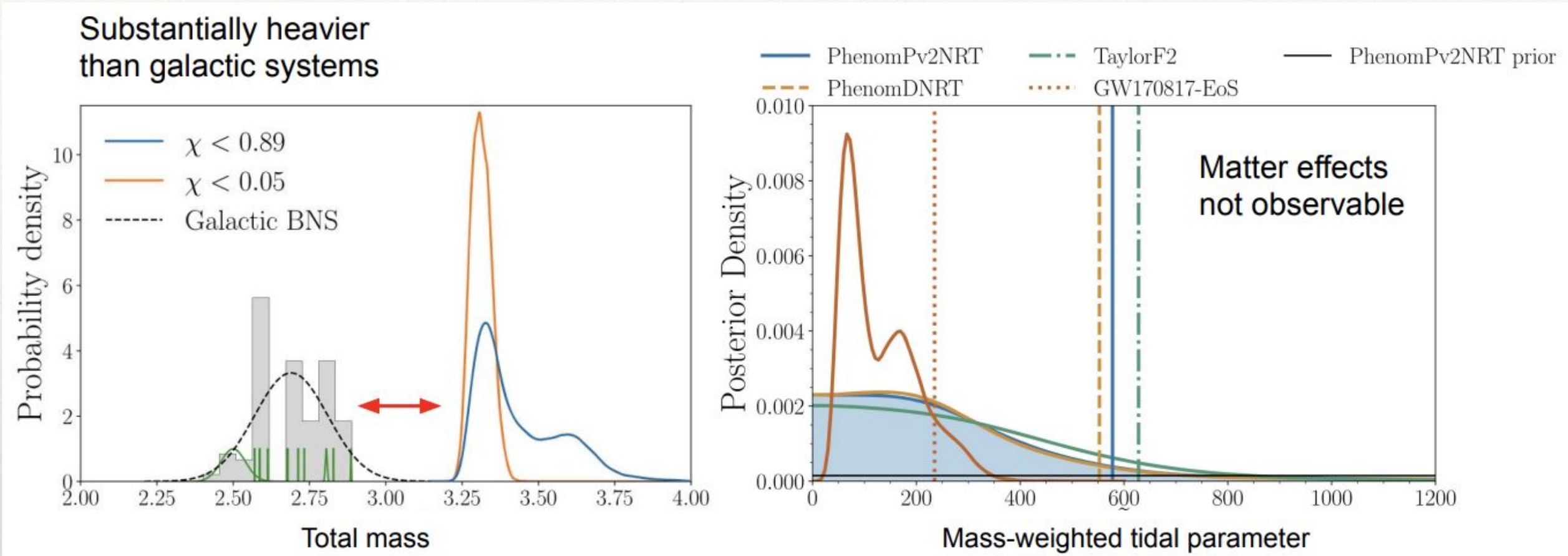

- Potentially BNS merger: no constraint of tidal parameter
- Heavier than typical Galactic BNSs: dynamical formation?
- Bad localization
- Distance 0.16Gpc - 4 times further than GW170817

GW190521

LVC, 2020, GW190521

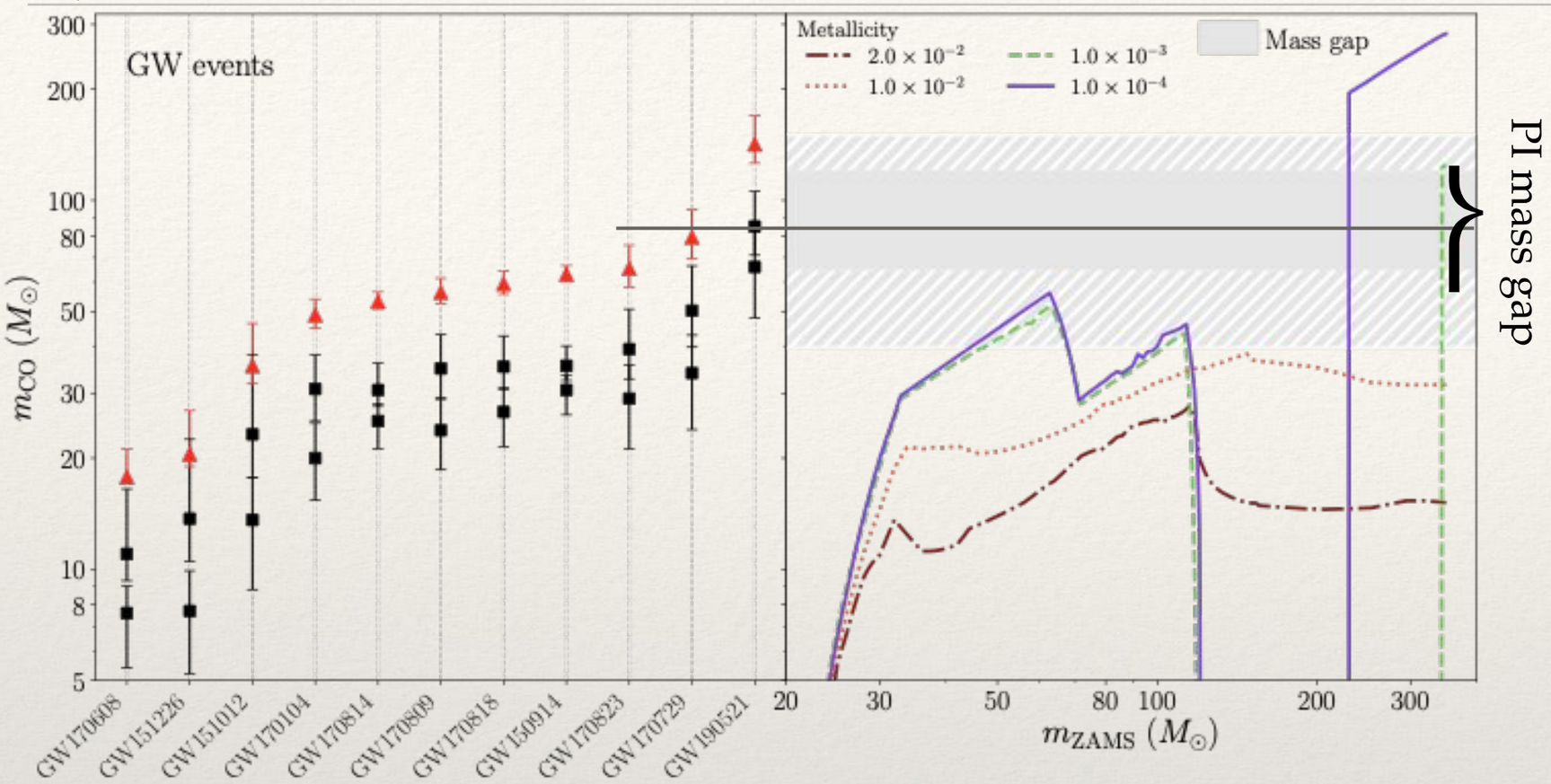

PI mass gap

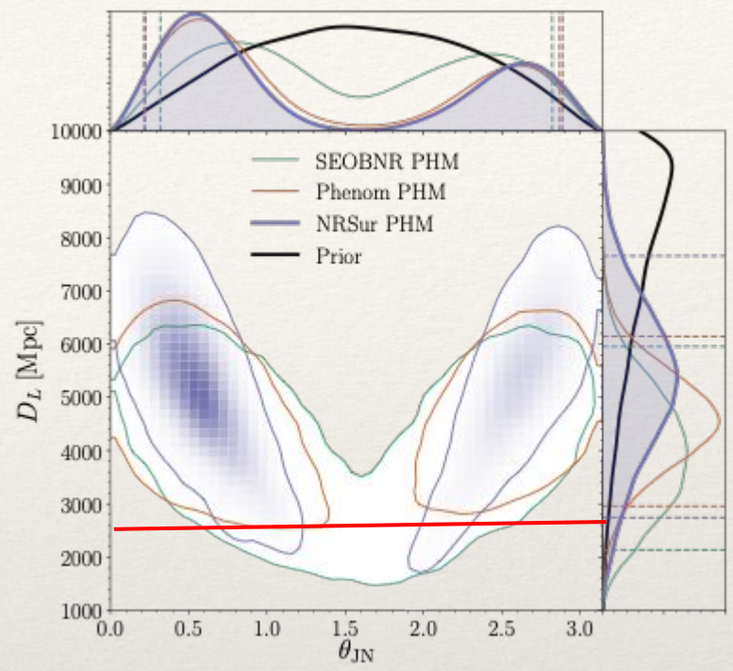

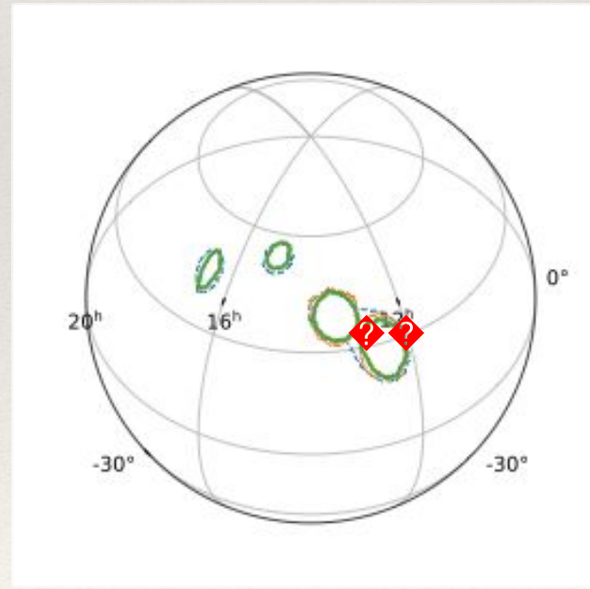

- Pair-Instability mass gap: production of electron-positron pairs in the stellar core softens the equation of state, removing pressure support
  - ignition of oxygen/silicon - explosion-like burning
  - pulsating instability: removing stellar envelope
- Above mass gap: direct collapse to BH

- Zwicky Transient Facility observed an optical flare (ZTF19abanrhr), interpreted as coming from the kicked GW190521 BH merger remnant moving in an AGN disk

GW190814

LVC, 2020, GW190814

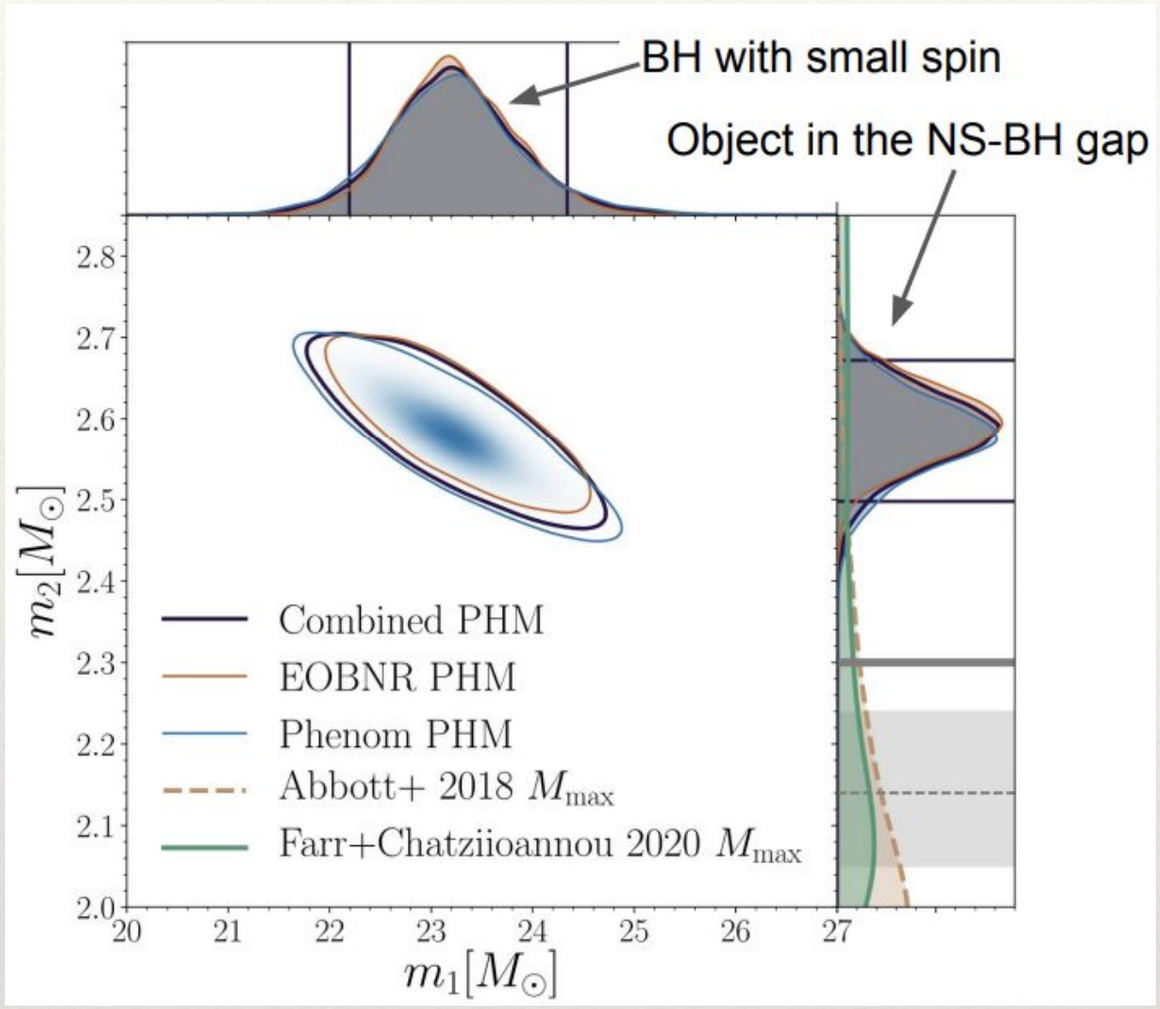

- Lightest BH? could be...
- Heaviest NS?
  - rapid rotation, stiff EOS
- Exotic object?

- Source parameters: $m_2 = 2.6\ M_{solar}$, q=0.11
- Best localization: 19 deg^2, $V_{90\%} = 3.2 \times 10^{-5}\ Gpc^3$
- Challenges in formation of such system

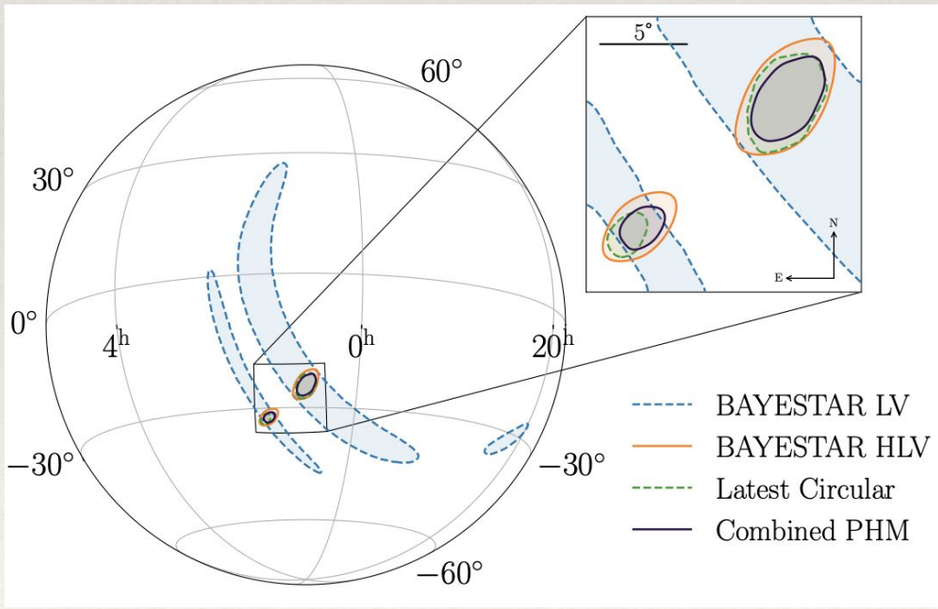

Summary

- We have reported on 39 new GW events from O3a (1 Apr 2019 - 1 Oct 2019): to be added to 11 events reported from O1-O2
- Three binaries with $m_2 < 3M_{solar}$: might include first BHNS
- Several interesting "special cases" including compact objects in lower and upper mass gap
- Merging BHs in GWTC2 are more massive and further away
- Very mild evidence for precession, but strong evidence for higher order modes in asymmetric binaries